

1982

Vibration Analysis of Rotary Compressors

K. Imaichi

M. Fukushima

S. Muramatsu

N. Ishii

Follow this and additional works at: <https://docs.lib.purdue.edu/icec>

Imaichi, K.; Fukushima, M.; Muramatsu, S.; and Ishii, N., "Vibration Analysis of Rotary Compressors" (1982). *International Compressor Engineering Conference*. Paper 407.
<https://docs.lib.purdue.edu/icec/407>

This document has been made available through Purdue e-Pubs, a service of the Purdue University Libraries. Please contact epubs@purdue.edu for additional information.

Complete proceedings may be acquired in print and on CD-ROM directly from the Ray W. Herrick Laboratories at <https://engineering.purdue.edu/Herrick/Events/orderlit.html>

Vibration Analysis of Rotary Compressors

Kensaku Imaichi: Professor, Osaka University, Toyonaka, Osaka 560, Japan,
 Masafumi Fukushima: Chief Engineer, Matsushita Electric Industrial Co., Ltd.
 (PANASPNIC), Nojicho, Kusatsu 525, Japan,
 Shigeru Muramatsu: Chief Engineer, Matsushita Electric Industrial Co., Ltd.,
 Noriaki Ishii: Professor, Osaka Electro-Communication University, Neyagawa,
 Osaka 572, Japan.

ABSTRACT

By theoretically analyzing dynamic behavior of the crankshaft, the rolling piston and the blade in rolling-piston rotary compressors, constraint forces and sliding speed at each pair of movable machine elements were obtained, and unbalanced inertia forces and compressor vibrations were evaluated. It was concluded that theoretical results have a good agreement with experimental ones. Moreover, it was revealed that one of major factors which cause compressor vibrations is speed variation of the crankshaft and compressor vibrations are not affected by rolling behavior of the piston.

INTRODUCTION

Rolling-piston rotary compressors have the advantages

of high volumetric efficiency and small mechanical loss and they are compact and light in weight, compared to corresponding reciprocating compressors [1-4]. In rotary compressors, moreover, vibrations are comparatively small in amplitude as they have few reciprocating elements, and hence have been considered suitable for lowering the noise in air-conditioning equipment. Due to these properties, most air-conditioning compressors presently used in Japan are of the rolling-piston rotary type. It is likely that the popularity of rolling-piston compressors will continue to increase, and at the same time strong demands for reducing vibration and noise which arise from the compressors will also rise. To cope with these demands, unbalanced inertia forces due to the motion of machine elements, and vibrations caused by those forces have to be evaluated before a design which reduces the revealed vibrations most effectively can

Nomenclature

$a = 1/2$ of blade thickness $b =$ contact length of blade & cylinder $B =$ equivalent length of plain bearing $c =$ clearance of piston & crankpin $c_s =$ clearance of crankshaft & bearing $[C] =$ damping coefficient matrix $c_f, c_{fc}, c_{fs}, c_{pc} =$ friction & pressure constant of oil film $e =$ eccentricity of piston center $[E] =$ transfer matrix $[F] =$ exciting force matrix $f_1, f_2 =$ functions of θ $F_a =$ frictional force on piston $F_{cn}, F_{ct} =$ constraint & frictional forces on piston & cylinder $F_d =$ frictional force on blade ends $F_{en} =$ force on piston & crankpin $F_{gx}, F_{gy} =$ constraint forces on crankshaft & bearing $F_{gn1}, F_{gn2}, F_{gt1}, F_{gt2} =$ constraint & frictional forces on cylinder & blade $F_p =$ gas force on piston $F_{ps}, F_{pc} =$ gas forces on cylinder wall $F_{qx}, F_{qy} =$ gas forces on blade $F_s =$ spring force on blade $F_{vn}, F_{vt} =$ forces on blade & piston $F_x, F_y, F_z =$ exciting forces on cylinder center $h_{bu}, h_{bl} =$ height of balancers from cylinder center	$I_c =$ inertia moment of crankshaft $I_p =$ inertia moment of piston $I_X, I_Y, I_Z =$ inertia moment of comp. $k =$ spring constant $[K] =$ spring constant matrix $l =$ depth of cylinder $l_p =$ length of piston bearing $l_s =$ length of crank journal $M =$ mass of whole compressor $[M] =$ mass matrix $m_{bu}, m_{bl} =$ mass of balancers $m_c =$ total mass of crankpin, crank-arm & balancers $m_p =$ piston mass $m_v =$ blade mass $M_p =$ frictional moment on piston & crankpin $M_a =$ frictional moment on piston ends $M_m =$ motor torque $M_g =$ moment due to gas forces on blade $M_s =$ frictional moment on crankshaft & journal $M_x, M_y, M_z =$ moment on cylinder center $P_c, P_s =$ pressure in compression & suction chamber $P_d =$ pressure inside closed housing $R =$ cylinder radius $r, r_c =$ outside & inside piston radius $r_{bu}, r_{bl} =$ eccentricity of balancers	$r_s =$ radius of crankshaft $r_v =$ radius of blade tip $v_{Bn} =$ sliding speed of blade & piston $v_{pc} =$ sliding speed of piston & crankpin $[X] =$ displacement matrix $X, Y, Z =$ orthogonal coordinate $x, y, z =$ moving orthogonal coordinate $x_0, y_0, z_0 = X, Y, Z$ coordinate of cylinder center $X_G, Y_G, Z_G =$ parallel displacement $x_{oc}, y_{oc} =$ coordinate of m_c center $x_{op}, y_{op} =$ coordinate of piston center $x_v =$ variable of blade motion $\alpha =$ angle of \overline{OG}_2 & x axis $\gamma_1, \gamma_2, \gamma_3, \gamma_4, \gamma_5 =$ function of θ $\delta_{pb} =$ piston & blade ends clearance $\delta_{pc} =$ minimum clearance of piston & cylinder $\delta_1, \delta_2, \delta_3, \delta_4 =$ constant +1 or -1 $\epsilon =$ eccentricity of m_c gravity center $\eta =$ rotating angle of F_{en} $\eta_g =$ dynamic viscosity of R22 $\eta_o =$ dynamic viscosity of oil $\theta =$ rotating angle of crankshaft $\theta_{XG}, \theta_{YG}, \theta_{ZG} =$ rotational displacement $\mu_g, \mu_v =$ friction coefficient $\xi =$ angle of \overline{OvOp} & x axis $\phi =$ rotating angle of piston
--	--	--

be developed. In this paper, an analytical method to evaluate the vibrations is established, and the experimental confirmation is shown.

Movable machine elements in a rolling-piston compressor are the rotating crankshaft, the rolling piston and the reciprocating blade. Each machine element moves in connection with the others. Now, the blade motion is a function of the turning angle of the crankshaft, provided that the blade top moves in contact with the piston. In the case of the piston, however, its rotating motion is independent of the crankshaft motion and is determined by all frictional forces exerted on it. Therefore, both equations of the crankshaft motion and the piston motion have to be simultaneously solved to reveal the dynamic behavior of the movable machine elements.

First, in this study, the equations of motion of the movable machine elements are derived, and then they are applied to a small rolling-piston rotary compressor, and one concrete example in which the rotating behavior of the crankshaft and the piston is obtained by numerical calculation is shown. Secondly, the equations which represent unbalanced inertia forces caused by the movable machine elements are presented, and the characteristics of the unbalanced inertia forces and the compressor vibrations which they cause are revealed by numerical calculation. Furthermore, the obtained compressor vibrations are compared with experimental results, and a major factor inducing compressor vibrations is examined. Thirdly, the effect of the piston motion on the compressor vibrations is examined by comparing the approximate solutions to the problem of the vibrations obtained under an assumption that the rotating speed of the piston is zero with exact solutions obtained by precise analysis of the rotating motion of the piston.

ROLLING-PISTON ROTARY COMPRESSOR

Fig.1(a) shows the construction of a rolling-piston rotary compressor which is used for air-conditioners of the refrigerating capacity 1755 kcal/h. The motor stator and the cylinder block are fixed inside the closed housing which is suspended with three rubber springs on a base. The refrigerant (R22) is sucked into the cylinder through the accumulator. The compressed refrigerant is discharged inside the closed housing and transferred to a condenser through the discharge pipe on the top of the closed housing. The dimensions of the closed housing are 110 mm diameter and 212 mm high, and the mass of the whole compressor is 8.7 kg. The motor is a single phase induction motor. The synchronous speed is 3600 rpm and the power is 0.55 kW. The machine part compressing the refrigerant is soaked in the lubricating oil and the gas leakage from the compression chamber is prevented by oil sealing. Fig.1(b) shows the A-A' cross-section of the machine part. The machine part consists of the cylinder with bore 39 mm, the reciprocating blade with thickness 32 mm, the piston with outside diameter 32.5 mm and the crankshaft system which is composed of the crankshaft, the crankpin and the motor rotor. The eccentricity of the piston center O_p from the rotating crankshaft center O is 3.26 mm and the cylinder depth is 28 mm. The center axis of the blade coincides with the cylinder center O and the blade tip with radius 3.2 mm is pushed on the piston by the spring force and the gas force which are

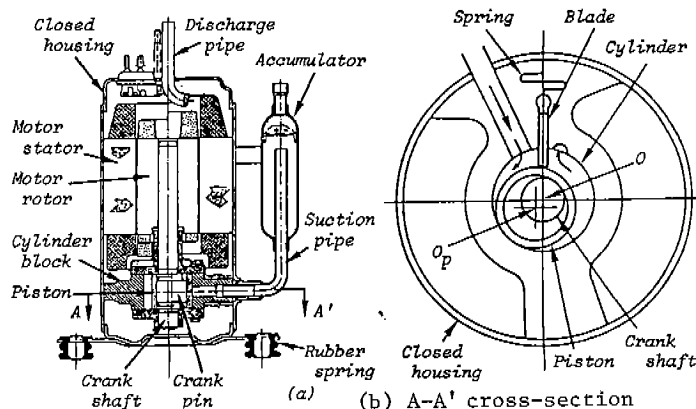


Fig.1 Construction of Rolling-Piston Compressor

exerted on the back end. The minimum value of the piston-cylinder wall clearance is about $10 \mu\text{m}$. The piston-crankpin clearance is about $20 \mu\text{m}$ and this pair is lubricated by an oil pump attached to the lower end of the crankshaft. The arrows shown in the figure express the direction of the refrigerant gas flow. The refrigerant is sucked in the suction chamber and discharged inside the closed housing after compressed in the compression chamber.

EQUATION OF MOTION OF MOVABLE MACHINE ELEMENTS

Coordinate and Variables

To reveal unbalanced inertia forces which cause the compressor vibrations, the equations of the crankshaft system, the piston and the blade have to be derived. For this purpose, the orthogonal coordinate and the variables are defined as shown in Fig.2. The x, y, z coordinate is fixed on the cylinder. The origin coincides with the cylinder center O , the x axis with the blade center line and the z axis with the crankshaft center. The main variables are the turning angle θ of the crankshaft and the rotating angle ϕ of the piston. The distance x_v of the blade tip center O_v and the cylinder center O and the angle ξ of the line $O_v O_p$ are defined as ancillary variables.

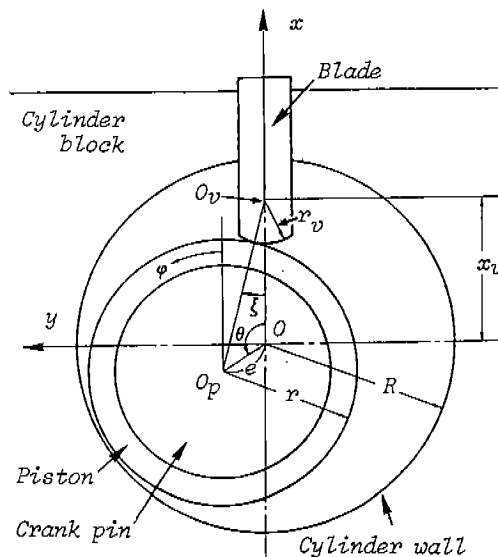


Fig.2 Coordinate and Variables

θ and ϕ are defined as positive when counterclockwise turn and ξ positive when clockwise turn. Assuming that the blade reciprocates in contact with the piston, the ancillary x_v and ξ is given by the following relations.

$$(r_v+r)\sin\xi = ex\sin\theta \quad (1)$$

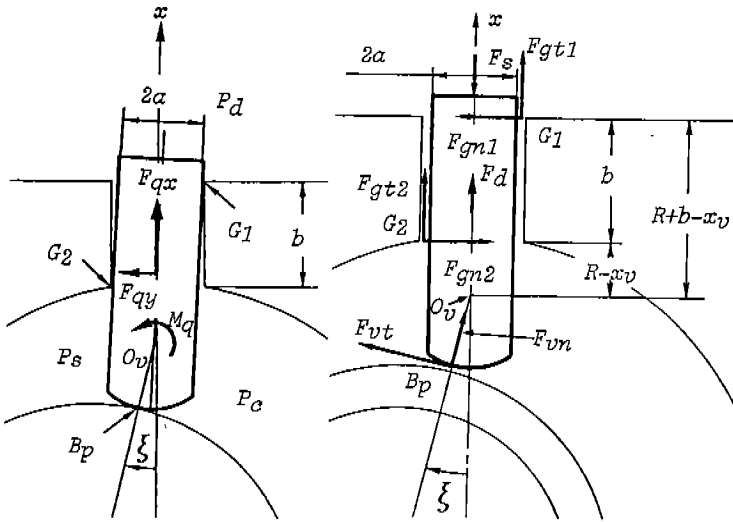
$$x_v = (r_v+r)\cos\xi + e\times\cos\theta \quad (2)$$


Fig.3 Gas Forces and Moment Exerted on the Blade

Equations of Motion of Blade

It is supposed that as shown in Fig.3, the blade center line slightly tilts in the clockwise direction, since the blade is pushed by the comparatively high pressure P_c in the compression chamber. Therefore, the blade contacts with the cylinder at G_1 and G_2 points shown in the figure. Hence, the blade surface from G_1 to the contact point B_p with the piston is pushed by the gas pressure P_c , the surface from B_p to G_2 by the gas pressure P_s in the suction chamber and the surface from G_2 to G_1 by the mean gas pressure P_d inside the closed housing. The x and y components F_{qx} , F_{qy} of the resultant gas force exerted on the blade and the counterclockwise moment M_q about O_v which is caused by the following forms, respectively.

$$F_{qx} = \{-2aP_d + (a+r_v)\sin\xi\}P_c + \{a-r_v\sin\xi\}P_s\}l,$$

$$F_{qy} = \{-bP_d + (R+b-x_v+r_v\cos\xi)P_c - (R-x_v+r_v\cos\xi)P_s\}l,$$

$$M_q = [-b(R-x_v+b/2)P_d + \{(R+b-x_v)^2 + a^2 - r_v^2\}P_c/2 - \{(R-x_v)^2 + a^2 - r_v^2\}P_s/2]l \quad (3)$$

Furthermore, many forces shown in Fig.4 exerted on the blade. The constraint forces F_{gn1} , F_{gn2} , F_{vn} and the frictional forces F_{gt1} , F_{gt2} , F_{vt} arise at G_1 , G_2 and B_p points, respectively in the directions shown in the figure. The following spring force F_s and the frictional force F_d due to the oil viscosity:

$$F_s = k(x_v - r + e) \quad (4) \quad F_d = \text{sgn}(-\dot{x}_v)\eta_0\dot{x}_v/\delta_{pb} \quad (5)$$

exert on the back end and the upper & lower ends respectively. Considering all forces exerted on the blade, the equation of the reciprocating motion:

$$m_v\ddot{x}_v = -F_s + F_{qx} + F_{gt1} + F_{gt2} + F_{vn}\cos\xi + F_{vt}\sin\xi + F_d \quad (6)$$

is obtained, and the equilibrium equation of the forces in the y direction and that of the moment about O_v point are respectively given by the following

forms.

$$F_{qy} + F_{vt}\cos\xi - F_{vt}\sin\xi + F_{gn1} + F_{gn2} = 0 \quad (7)$$

$$(R+b-x_v)F_{gn1} + aF_{gt1} - (R-x_v)F_{gn2} - aF_{gt2} + M_q - r_vF_{vt} = 0 \quad (8)$$

Since it is considered that the frictional state at the blade-cylinder pair and the blade-piston pair is under the boundary lubrication, the frictional forces F_{gt1} , F_{gt2} , F_{vt} at G_1 , G_2 and B_p points are subject to Coulomb's law of friction.

$$F_{gt1} = \text{sgn}(-\dot{x}_v)\mu_g|F_{gn1}|, \quad F_{gt2} = \text{sgn}(-\dot{x}_v)\mu_g|F_{gn2}|, \quad F_{vt} = \text{sgn}(v_{Bn})\mu_vF_{vn} \quad (9)$$

where, v_{Bn} represents the sliding speed of the piston and the blade tip, and it is given by the following form:

$$v_{Bn} = r\dot{\phi} - e\dot{\theta}\cos(\theta+\xi) - r_v\dot{\xi} \quad (10)$$

When the frictional forces are evaluated by the equation (9), the constraint forces F_{gn1} , F_{gn2} , F_{vn} are given by the following matrix form which is derived from (6)-(9).

$$\begin{bmatrix} F_{gn1} \\ F_{gn2} \\ F_{vn} \end{bmatrix} = [A]^{-1} \begin{bmatrix} m_v\ddot{x}_v + F_s - F_{qx} - F_d \\ -F_{qy} \\ -M_q \end{bmatrix} \quad (11)$$

where, $[A]$ is the inverse matrix of the following matrix $[A]$.

$$[A] = \begin{bmatrix} \delta_1\delta_2\mu_g & \delta_1\delta_3\mu_g & \cos\xi + \delta_4\mu_v\sin\xi \\ 1 & -1 & \delta_4\mu_v\cos\xi - \sin\xi \\ R+b-x_v + \delta_1\delta_2a\mu_g & -R-x_v - \delta_1\delta_3a\mu_g & -\delta_4r_v\mu_v \end{bmatrix} \quad (12)$$

in which $\delta_1, \delta_2, \delta_3, \delta_4$ represent constants given by the following definitions.

$$\delta_1 = \text{sgn}(-\dot{x}_v), \delta_2 = \text{sgn}(F_{gn1}), \delta_3 = \text{sgn}(F_{gn2}), \delta_4 = \text{sgn}(v_{Bn}) \quad (13)$$

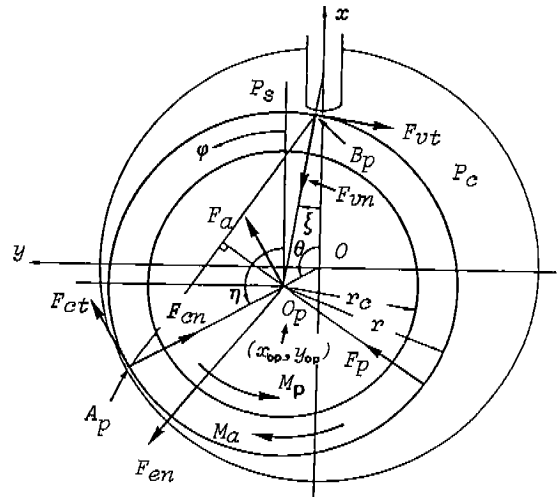


Fig.5 Forces and Moment on the Piston

Equations of Motion of the Piston

Fig.5 shows the forces and the moment exerted on the piston. The point A_p shows the position of the minimum clearance between the piston and the cylinder wall. The blade and the point A_p divide the cylinder into the compression chamber and the suction one. The resultant gas force F_p exerted on the piston is given by the following equation.

$$F_p = 2r\sin\{(\theta+\xi)/2\} \times l(P_c - P_s) \quad (14)$$

The direction of F_p is perpendicular to the line \overline{ApBp} and passes the piston center O_p . The forces F_{vn} and F_{vt} given by (11) exert on the contact point B_p with the blade, in the directions shown in the figure respectively. The gap of the piston and the crankpin is lubricated by the oil pump, and so it is considered that the frictional state at this gap is evaluated by Sommerfeld's lubrication theory of journal bearing [5]. Hence, the frictional moment M_p exerted on the inside surface of the piston is given by the following form.

$$M_p = C_f \eta_0 r_c^2 v_{pc} l_p / C \quad (15)$$

where, v_{pc} represents the sliding speed of the piston and the crankpin, and is defined by the following form.

$$v_{pc} = r_c (\dot{\theta} - \dot{\phi}) \quad (16)$$

Furthermore, the resultant F_{en} of the oil film force exerts on the inside surface of the piston. The direction of F_{en} passes the piston center O_p and is expressed by the turning angle η from the x axis. Considering that Reynolds' lubrication theory of plane bearing [6] is applicable to the refrigerant flow near the point A_p , the frictional force F_{ct} and the gas film force F_{en} are evaluated by the following forms.

$$F_{ct} = C_f c \eta_0 B e / \delta_{pc} \times \dot{\theta}, \quad F_{en} = C_{pc} \eta_0 B^2 e / \delta_{pc}^2 \times \dot{\theta} \quad (17)$$

Moreover, the following frictional force F_a and moment M_a which are caused by the oil viscosity exert on the upper and lower ends of the piston, in the directions shown in the figure respectively.

$$F_a = 2\pi \eta_0 (r^2 - r_c^2) / \delta_{pb} \times \dot{\theta},$$

$$M_a = \pi \eta_0 (r^4 - r_c^4) / \delta_{pb} \times \dot{\phi} \quad (18)$$

Considering all forces exerted on the piston, the equilibrium equations of the forces in the x and y directions are given by the following forms.

$$-m_p \ddot{x}_{op} + F_{en} \times \cos \eta - F_{vn} \times \cos \xi - F_{vt} \times \sin \xi - F_{cn} \times \cos \theta + F_{ct} \times \sin \theta + F_p \times \cos \{(\theta - \xi) / 2\} + F_a \times \sin \theta = 0 \quad (19)$$

$$-m_p \ddot{y}_{op} + F_{en} \times \sin \eta + F_{vn} \times \sin \xi - F_{vt} \times \cos \xi - F_{cn} \times \sin \theta - F_{ct} \times \cos \theta + F_p \times \sin \{(\theta - \xi) / 2\} - F_a \times \cos \theta = 0 \quad (20)$$

where (x_{op}, y_{op}) represents the coordinate of the piston center O_p and they are defined by $x_{op} = e \times \cos \theta$, $y_{op} = e \times \sin \theta$. From the above equations (19) and (20), the oil film force F_{en} and its direction η are obtained by the following forms.

$$F_{en} = \sqrt{f_1^2 + f_2^2},$$

$$\eta = \tan^{-1}(f_2 / f_1) \quad (21)$$

where, the functions f_1 and f_2 of θ are defined as follows.

$$f_1 = (\cos \xi + \delta_4 \mu_v \times \sin \xi) F_{vn} + (C_{pc} B / \delta_{pc} \times \cos \theta - C_f c \times \sin \theta) \eta_0 B e / \delta_{pc} \times \dot{\theta} - F_p \times \cos \{(\theta - \xi) / 2\} - F_a \times \sin \theta - m_p e (\dot{\theta}^2 \times \cos \theta + \ddot{\theta} \times \sin \theta),$$

$$f_2 = (-\sin \xi + \delta_4 \mu_v \times \cos \xi) F_{vn} + (C_{pc} B / \delta_{pc} \times \sin \theta + C_f c \times \cos \theta) \eta_0 B e / \delta_{pc} \times \dot{\theta} - F_p \times \sin \{(\theta - \xi) / 2\} + F_a \times \cos \theta + m_p e (-\dot{\theta}^2 \times \sin \theta + \ddot{\theta} \times \cos \theta) \quad (22)$$

Moreover, considering the equilibrium of the moment about the piston center O_p , the equation of rotating motion of the piston takes the following form.

$$I_p \ddot{\phi} = r (F_{vt} + F_{ct}) + M_p - M_a \quad (23)$$

Equation of Motion of the Crankshaft

As shown in Fig.6, the motor torque M_m exerts on the crankshaft in the counterclockwise direction. On the other hand, the oil film force F_{en} exerts on the crankpin in the direction shown in the figure, and the frictional moment M_p given by (15) exerts in the clockwise direction, provided that the Sommerfeld variable of the oil film takes a fairly large value. The con-

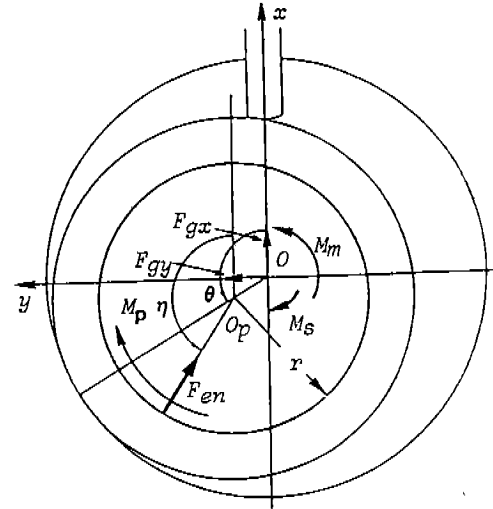


Fig.6 Forces and Moment on the Crankshaft

straint forces F_{gx} and F_{gy} exerts on the crankshaft center. From the equilibrium equations of the forces exerted on the crankshaft, F_{gx} and F_{gy} are given by the following forms.

$$F_{gx} = m_c \ddot{x}_{oc} + F_{en} \times \cos \eta, \quad F_{gy} = m_c \ddot{y}_{oc} + F_{en} \times \sin \eta \quad (24)$$

where, (x_{oc}, y_{oc}) represents the coordinate of the gravity center of the crankpin, the crank arm and balancers, and they are defined by the equations:

$x_{oc} = -e \cos \theta$, $y_{oc} = -e \sin \theta$. Since the gap of the crankshaft and the bearing is lubricated by the oil pump, the frictional moment M_s exerted on the crankshaft is evaluated by the following form, based on Sommerfeld's lubrication theory.

$$M_s = C_f s \eta_0 r_s^3 l_s \dot{\theta} / C_s \quad (25)$$

From the equilibrium of the moment about the crankshaft center, the equation of rotating motion of the crankshaft is obtained by the following form.

$$I_c \ddot{\theta} = M_m - e F_{en} \times \sin(\eta - \theta) - M_p - M_s \quad (26)$$

Eliminating F_{en} and η in the above equation by making use of (19) and (20), the equation (26) takes the following form.

$$(I_c + m_p e^2) \ddot{\theta} = M_m + e F_{vn} \times \sin(\theta + \xi) - e F_{vt} \times \cos(\theta + \xi) - e F_{ct} - e F_p \times \sin\{(\theta + \xi) / 2\} - e F_a - M_p - M_s \quad (27)$$

The second and third terms in the right hand side of the above equation represent the moment due to the constraint and frictional forces at the blade-piston pair, and they contain inertia terms caused by the reciprocating motion of the blade. Deriving the inertia terms by making use of (9) and (11), the above expression is arranged as follows:

$$\{I_c + m_p e^2 + m_v e^2 r_1(\theta) \times r_2(\theta)\} \ddot{\theta} = M_m - m_v e^2 \dot{\theta}^2 r_1(\theta) \times r_3(\theta) - r_1(\theta) e (F_{qx} + F_d - F_s) - r_4(\theta) e F_{qy} + r_5(\theta) M_a - e F_{ct} - e F_p \times \sin\{(\theta + \xi) / 2\} - e F_a - M_p - M_s \quad (28)$$

where, the functions $\gamma_1, \gamma_2, \gamma_3, \gamma_4, \gamma_5$ of θ is defined as follows: $r_1(\theta) = \{\sin(\theta + \xi) - \delta_4 \mu_v \times \cos(\theta + \xi)\} \times \{\delta_1(\delta_2 - \delta_3) \mu_g a + b\} / |A|$, $r_2(\theta) = \{1 + e / (r + r_v) \times \cos \theta / \cos \xi\} \times \sin \theta$, $r_3(\theta) = \{1 + e / (r + r_v) \times \cos \theta / \cos \xi\} \times \cos \theta + e / (r + r_v) \times \{e / (r + r_v) \times \cos^2 \theta / \cos \xi \times \tan \xi - \sin \theta\} \times \sin \theta / \cos \xi$, $r_4(\theta) = \{\sin(\theta + \xi) - \delta_4 \mu_v \times \cos(\theta + \xi)\} \{(\delta_2 + \delta_3)(R - x_v) + 2\delta_1 \delta_2 \delta_3 \mu_g a$

$$+\delta_3 b \delta_1 u_g / |A|, r_5(\theta) = e \{ \sin(\theta + \xi) - \delta_4 \times \mu_v \times \cos(\theta + \xi) \} \delta_1 (\delta_2 + \delta_3) u_g / |A|, \quad (29)$$

Unbalanced Inertia Forces and Equations of Vibrations

To examine the compressor vibrations, as shown in Fig.7, all forces and moment exerted on the cylinder block and the crank journal have to be clarified. The cylinder pressure P_s and P_c push the cylinder wall. The resultant forces F'_{ps} and F'_{pc} is given by the expressions:

$$F'_{ps} = 2R \sin\{(\theta - \alpha)/2\} \times LP_s, \\ F'_{pc} = 2R \sin\{(\theta + \alpha)/2\} \times LP_c \quad (30)$$

and the directions of F'_{ps} and F'_{pc} pass the cylinder center O and are perpendicular to the line ApG_2 and ApG_3 respectively. Furthermore, the constraint forces F_{gn1}, F_{gn2}, F_{cn} , the frictional forces $F_{gt1}, F_{gt2}, F_d, F_{ct}, F_a$ and the spring force F_s exert on the cylinder block in the directions shown in the figure respectively. The moment M_m as the reaction force to the motor torque exerts on the cylinder block in the clockwise direction. The oil film forces F_{gx}, F_{gy} and the frictional moment M_s exert on the crankshaft in the directions shown in the figure respectively.

Arranging the total of all forces and moment exerted on the cylinder block and the crank journal, the x, y, z components F_x, F_y, F_z of the resultant force on the cylinder center O and the moment M_x, M_y, M_z about x, y, z axis take the following forms of the unbalanced inertia forces.

$$F_x = -m_v \ddot{x}_v + (m_p e - m_c e) (\dot{\theta}^2 \times \cos\theta + \ddot{\theta} \times \sin\theta), \\ F_y = (m_p e - m_c e) (\dot{\theta}^2 \times \sin\theta - \ddot{\theta} \times \cos\theta), \\ F_z = 0, \\ M_x = (m_{bu} r_{bu} h_{bu} - m_{bl} r_{bl} h_{bl}) (\dot{\theta}^2 \times \sin\theta - \ddot{\theta} \times \cos\theta), \\ M_y = (m_{bu} r_{bu} h_{bu} - m_{bl} r_{bl} h_{bl}) (\dot{\theta}^2 \times \cos\theta + \ddot{\theta} \times \sin\theta), \\ M_z = -(I_c + m_p e^2) \ddot{\theta} - I_p \ddot{\phi} \quad (31)$$

where, M_x and M_y in the above equations are the moment caused by the mass m_{bu} and m_{bl} of the balancers which are attached to the upper and lower ends of the motor rotor respectively.

To represent the compressor vibrations, the X, Y, Z coordinate system is defined, in which the origin coincides with the compressor gravity center G at rest and the each axis is parallel to the corresponding axis of the x, y, z coordinate system. In this case, the compressor vibrations are subject to the following matrix equation.

$$[M][\ddot{X}] + [C][\dot{X}] + [K][X] = [E][F] \quad (32)$$

where, the displacement matrix $[X]$ of the gravity point G , the mass matrix $[M]$, the transfer matrix $[E]$ determined by the coordinate (x_0, y_0, z_0) of the cylinder center O , and the exciting force matrix $[F]$ composed of the unbalanced inertia forces are respectively defined as follows:

$$[X] = \begin{bmatrix} X_G \\ Y_G \\ Z_G \\ \theta_{XG} \\ \theta_{YG} \\ \theta_{ZG} \end{bmatrix}, \quad [M] = \begin{bmatrix} M & \cdot & \cdot & \cdot & \cdot & \cdot \\ \cdot & M & & & & \\ \cdot & & I_X & & & \\ \cdot & & & I_Y & & \\ 0 & \cdot & \cdot & \cdot & \cdot & I_Z \end{bmatrix},$$

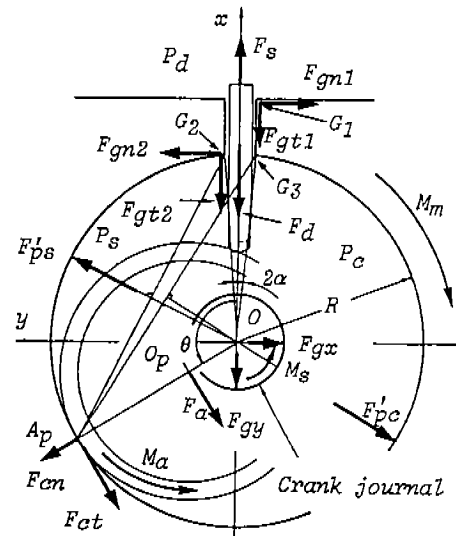


Fig.7 Forces and Moment on the Cylinder Block and the Crank Journal

$$[E] = \begin{bmatrix} 1 & \cdot & \cdot & \cdot & \cdot & \cdot & 0 \\ 0 & 1 & & & & & \\ 0 & 0 & 1 & & & & \\ 0 & -z_0 & y & 1 & & & \\ z_0 & 0 & -x_0 & 0 & 1 & & \\ -y_0 & x_0 & 0 & 0 & 0 & 1 & \end{bmatrix}, \quad [F] = \begin{bmatrix} F_x \\ F_y \\ F_z \\ M_x \\ M_y \\ M_z \end{bmatrix} \quad (33)$$

The matrices $[C]$ and $[K]$ are determined by viscosity coefficients and spring constants of the suspension system.

COMPUTER SIMULATION

Rotatory Behavior of the Crankshaft and the Piston

The rotatory behavior of the crankshaft and the piston is subject to the equations (28) and (23) respectively, and from these two equations the solutions θ and ϕ are obtained by computer calculation. The left term of (28) represents inertia terms and the right terms represent the driving torque and various loads which are functions of $\theta, \dot{\theta}$ and ϕ . Therefore, the equation (28) is arranged to the following expression.

$$\ddot{\theta} = f_c(\theta, \dot{\theta}, \phi) \quad (34)$$

The left term of (23) represent the inertia term of the rotating piston and the right terms are functions of $\theta, \dot{\theta}, \phi$ and $\ddot{\theta}$. Hence, the equation (23) is arranged to the following expression.

$$\ddot{\phi} = f_p(\theta, \dot{\theta}, \ddot{\theta}, \phi) \quad (35)$$

The solutions θ and ϕ which simultaneously satisfy (34) and (35) are numerically obtained by a method of repeated calculation. Since the piston speed $\dot{\phi}$ is fairly small compared with the crankshaft speed $\dot{\theta}$, first in this study, the crankshaft behavior is calculated from (34) under the assumption $\dot{\phi} = 0$, and on substitution of the obtained solutions $\theta, \dot{\theta}, \ddot{\theta}$ into (35), the piston behavior is calculated. Furthermore, on substitution of the obtained solutions $\dot{\phi}$ into (34), the higher order approximate solutions are calculated.

Tab.1 shows the mechanical constants of the compressor

chosen as the subject of this study. The gravity center and the inertia moment of the whole compressor are measured by applying the principle of rigid pendulum, and the accuracy of the measurement is better than about 2%. Fig.8 shows the motor torque characteristics. The synchronous speed is 3600 rpm and the maximum torque is 3.4 N·m when 2780 rpm. Fig.9 shows the compression and suction gas pressure P_c and P_s when the compressor is operated under a standard load (the mean discharged pressure inside the closed housing $P_d = 2.06$ MPa, the mean suction pressure = 0.54 MPa). In this standard load, the average speed of the crankshaft is 358.8 rad/s (3425.8 rpm). The abscissa of Fig.9 represents the elapsed time and the time $t = 0$ corresponds the crank angle $\theta = 0$. The periodic time for one revolution of the crankshaft is 17.51 ms. The gas pressure P_c has two peaks. The first peak is slightly larger than the second and the first peak value is 2.41 MPa. The minimum value of P_c is 0.48 MPa. The lubricating oil is SUNISO 4GF (Sun Oil Co., Ltd.) and it is supposed that the dynamic viscosity takes the value 2.076 mPa·s when the pressure is 2 MPa, the temperature 100 °C and the mass percent R-22 in the oil 15%. It is assumed that the dynamic viscosity η_g of the refrigerant takes the value 16.9 μ Pa·s for the above pressure and temperature. Since it is so designed that the bearing loads at the piston-crankpin pair and the crankshaft-bearing pair are comparatively small, it is considered that the Sommerfeld's variables at these pairs take fairly larger values than 1.0. Hence, the eccentricity rate of the shaft center is lower than about 1.0% and then the friction constants C_f and C_{fs} take the value of 2π . It is supposed that the frictional force F_{ot} of the refrigerant gas film near the minimum clearance between the piston and the cylinder wall is calculated by considering that $C_{fc}B/\delta_{pc}$ approaches about 170 when the equivalent length B of plane bearing becomes larger than about 5.5 mm.

When the frictional coefficients μ_g and μ_v at the blade-cylinder block pair and at the piston-blade pair respectively are given in addition to the above mentioned conditions, the rotatory behavior of the crankshaft and the piston is determined from (34) and (35). In this study, it is assumed that the values of μ_g and μ_v are equal, and a method to determine the value so as to satisfy an energy equation derived from the equation(28) is adopted. When the equations (34) and (35) are computer simulated by dividing the period time 17.51 ms into the 180 equal steps, the calculated result of μ_g and μ_v was 0.04 which is reasonable for boundary lubrication. Fig.10 shows the rotatory behavior of the crankshaft and Fig.11 shows the piston behavior. The crankshaft speed $\dot{\theta}$ fluctuates from 371.8 rad/s to 343.9 rad/s, and hence the speed variation is about 7.8%. The angular acceleration $\ddot{\theta}$ fluctuates from -8687 rad/s² to 4667 rad/s² and the fluctuating p-p value is about 13350 rad/s². The sharp peak of $\ddot{\theta}$ at the time 2.0 ms correspond well to the first peak of P_c shown in Fig.9. When the time $t = 4.4$ ms and 12.1 ms, the angular acceleration $\ddot{\theta}$ rapidly changes like a step. The fluctuating p-p value of $\ddot{\theta}$ is about 13540 rad/s². Corresponding to these rapid changes of $\ddot{\theta}$, the piston speed $\dot{\phi}$ changes like a broken line, from -14.6 rad/s

Tab.1 Mechanical Constants

a mm	1.6	k N/cm	12.5	r_c cm	1.20
b cm	1.47	l cm	2.80	r_{bu} cm	1.16
C μ m	7.2	l_p cm	1.80	r_{bl} cm	1.25
C_s μ m	6.7	l_s cm	4.4	r_s mm	8.0
e mm	3.26	M kg	8.70	r_v mm	3.2
hb_u cm	1.39	m_{bu} kg	1.01×10^{-2}	x_0 mm	-4.3
hb_l cm	3.40	m_{bl} kg	5.19×10^{-2}	y_0 mm	-2.2
I_c N·cm·s ²	0.422	m_c kg	1.39×10^{-1}	z_0 cm	-6.54
I_p N·cm·s ²	1.53×10^{-3}	m_p kg	7.41×10^{-2}	α rad	8.21×10^{-2}
I_X N·cm·s ²	35.2	m_v kg	1.13×10^{-2}	δ_{pb} μ m	15
I_Y N·cm·s ²	39.0	R cm	1.95	δ_{pc} μ m	15
I_Z N·cm·s ²	10.0	r cm	1.62	ϵ mm	1.7

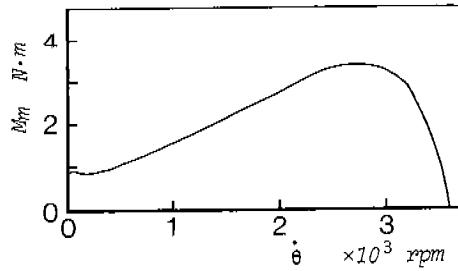


Fig.8 Motor Torque Characteristics

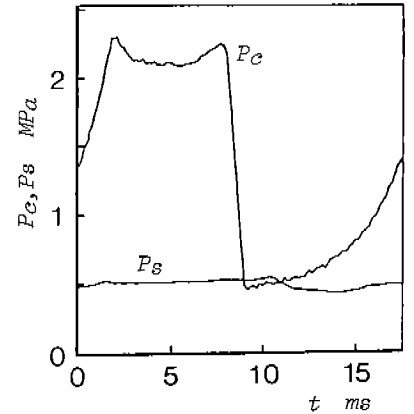


Fig.9 Compression and Suction Gas Pressure

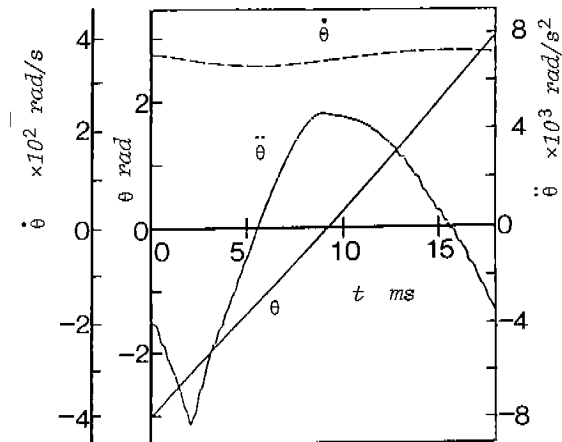


Fig.10 Rotatory Behavior of the Crankshaft

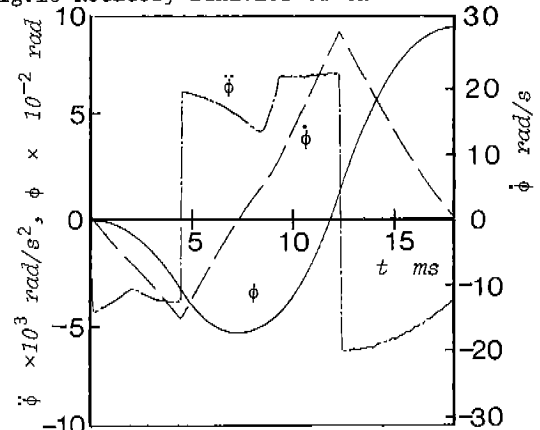


Fig.11 Rotatory Behavior of the Piston

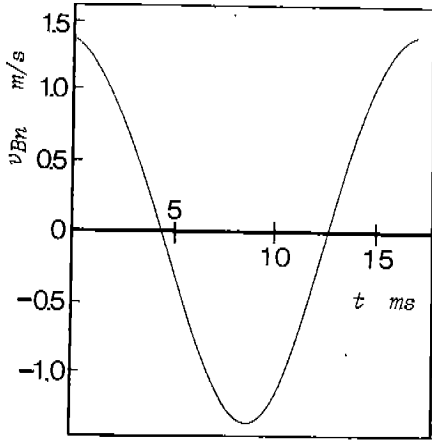


Fig.12 Sliding Speed v_{Bn}

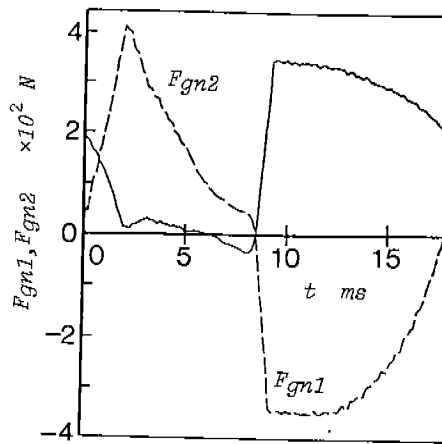


Fig.13 Constraint Forces F_{gn1}, F_{gn2}

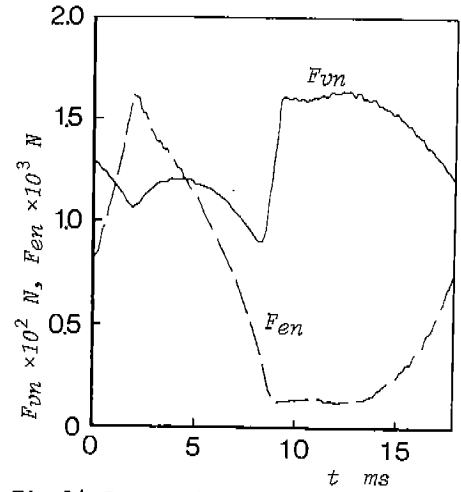
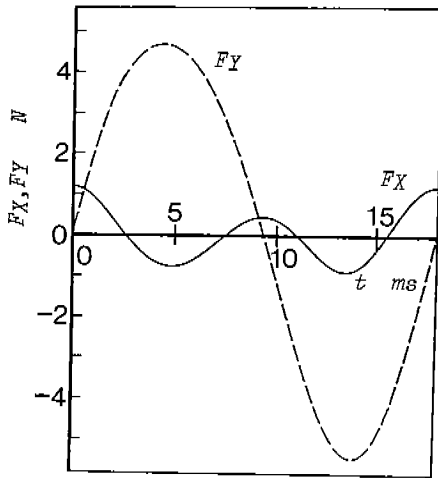
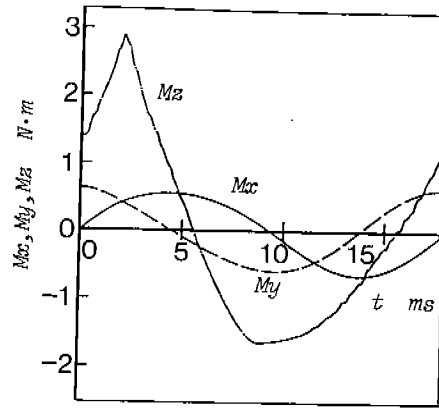


Fig.14 Constraint Forces F_{vn}, F_{en}



(a)



(b)

Fig.15 Unbalanced Inertia Forces on the Cylinder Center O

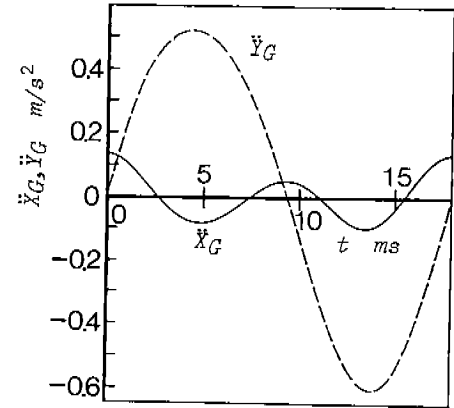
to $+29.0 \text{ rad/s}^2$. The time when the piston behavior rapidly changes correspond well to the instant when the directions of the sliding speed v_{Bn} of the piston and the blade changes, as shown in Fig.12.

Fig.13 shows the constraint forces F_{gn1}, F_{gn2} at the blade -cylinder block pair. F_{gn1} changes from -35 N to $+333 \text{ N}$, and F_{gn2} changes by about two times of F_{gn1} , that is, from -344 N to $+397 \text{ N}$. Fig. 14 shows the constraint forces F_{vn}, F_{en} at the blade-piston pair and at the piston-crankpin pair respectively. F_{vn} changes from $+90 \text{ N}$ to $+160 \text{ N}$ and so it is seen that the blade is tightly pushed on the piston. F_{en} has a sharp peak which corresponds to the first peak of P_c and changes from $+120 \text{ N}$ to 1580 N .

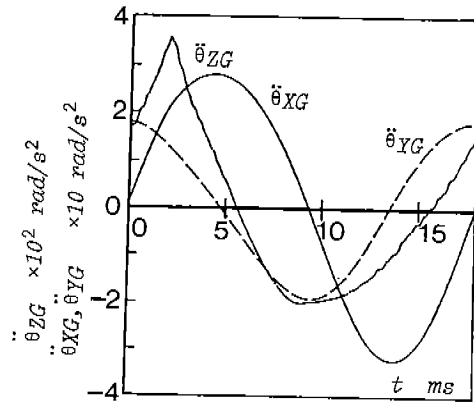
Unbalanced Inertia Forces and Compressor Vibration

On substitution of the obtained rotatory behavior of the crankshaft and the piston into (31), the unbalanced inertia forces shown in Fig.15 are clarified. F_x and F_y fluctuate from -0.8 N to $+1.2 \text{ N}$ and from -5.3 N to $+4.7 \text{ N}$ respectively, and so these fluctuating amplitudes are fairly small. The p-p values of M_x and M_y are about $1.50 \text{ N}\cdot\text{m}$. On the other hand, M_z changes from $-1.97 \text{ N}\cdot\text{m}$ to $+3.67 \text{ N}\cdot\text{m}$ and the p-p value is fairly large $5.64 \text{ N}\cdot\text{m}$.

When the natural frequency of the vibration system



(a)



(b)

Fig.16 Vibratory Acceleration of Compressor

is fairly small compared with the crankshaft speed, solutions of the vibration equation (32) are approximately obtained by the following expression.

$$[\ddot{X}] = [M]^{-1}[E][F] \quad (36)$$

On substitution of the inertia forces $[F]$ shown in Fig.15 into the above expression, the vibratory acceleration $[\ddot{X}]$ of the compressor gravity center is obtained, as shown in Fig.16. The p-p values of \ddot{X}_G and \ddot{Y}_G are fairly small 0.23 m/s^2 and 1.14 m/s^2 respectively. The p-p values of $\ddot{\theta}_{XG}$ and $\ddot{\theta}_{YG}$ are 60 rad/s^2 and 36 rad/s^2 respectively. On the other hand, the p-p value of $\ddot{\theta}_{ZG}$ is fairly large 567 rad/s^2 which is about ten times larger than those of $\ddot{\theta}_{XG}$ and $\ddot{\theta}_{YG}$. Comparing the wave form of $\ddot{\theta}_{ZG}$ with that of $\ddot{\theta}$

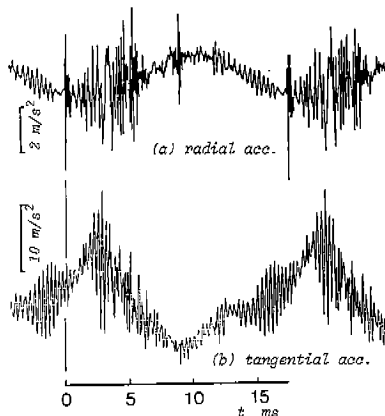


Fig.17 Measured Vibrations

shown in Fig.10, it is easily seen that this vibratory component with large amplitude was caused by the larger speed variation of the crankshaft.

COMPARISON OF CALCULATED RESULTS WITH EXPERIMENTAL RESULTS

To examine the calculated results, the compressor vibration on the cylindrical closed housing is measured and it is compared with the computer simulated results. The measured point is on the horizontal plane which passes the cylinder center O , and it has the coordinate (5.04, -2.10, -6.65 cm). The measured directions are the tangential and the normal (called 'radial') to the cylindrical shell, on the above horizontal plane. Fig.17 shows the experimental results, in which (a) shows the radial vibratory acceleration and (b) the tangential. The calculated results corresponding to the above experimental results are presented in Fig.18, in which the solid line shows the tangential acceleration \ddot{X}_{st} and the dotted line the radial \ddot{X}_{sr} . The calculated results cannot simulate the vibratory components of higher frequency, and it is seen that the measured vibration forms of the lower frequency are closely simulated by the computer calculation. Fig.19 shows a comparison of the vibration power spectrum. The abscissa is the frequency order and the fundamental frequency is 57.1 Hz. The ordinate is the vibration level expressed by decibel. 0 dB shows 1.0 m/s². The solid lines show the calculated results, and \circ sings show the power spectrum of the measured tangential acceleration which was analyzed by the first fourier translator (Nicolle-660). From this comparison, it is seen that the calculated results simulate precisely the measured vibration components which frequency order is lower than eight.

CONCLUSIONS

By exact analysis of the dynamic behavior of the movable machine elements in rolling-piston rotary compressors, a method of vibration analysis of the rotary compressors was presented, and it was applied to a small rolling-piston rotary compressor with a motor power of 550 W which is widely used for air-conditioners with the refrigerating capacity of 1755 kcal/h. The conclusions obtained in this study are as follows:

(1) The speed variation of the crankshaft was about 7.8 % and the fluctuating peak to peak value of the rotatory acceleration was 13350 rad/s². The fluctuating wave from of the rotatory acceleration was closely related to that of the gas pressure in the

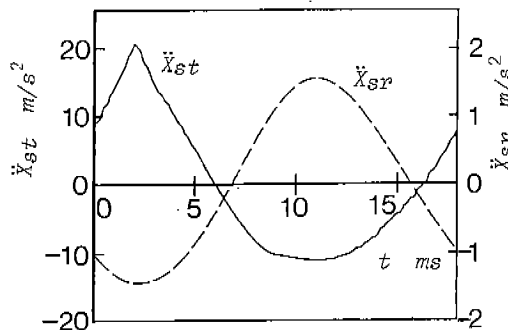


Fig.18 Calculated Vibrations

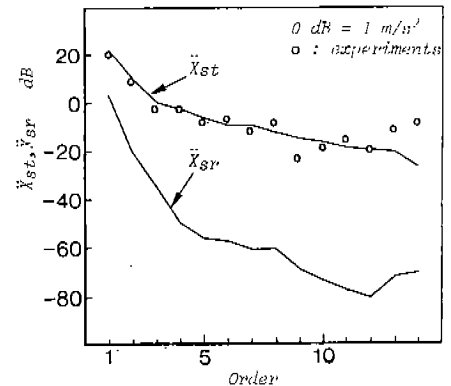


Fig.19 Power Spectrum

compression chamber. The rotatory acceleration of the piston rapidly changed at the time $t = 4.4$ ms and 12.1 ms when the direction of the sliding speed at the piston-blade pair changed, and the fluctuating value reached about 13540 rad/s².

(2) The characteristics of the fluctuating constraint forces were revealed, and hence fundamental design criteria for manufacturing compressors which are more compact and lighter in weight were obtained.

(3) The calculated results of the compressor vibrations were able to precisely simulate the measured vibration components which frequency order is lower than 8th. One major factor inducing compressor vibrations is an unbalanced inertia force based on the fairly large speed variation of the crankshaft and hence the vibration component about the crankshaft center is fairly large in amplitude compared with the other vibration components.

(4) When only the compressor vibrations are discussed, the analysis of the piston rotatory motion is negligible, since the inertia moment of the piston is fairly small compared with of the rotating crankshaft system in general. Hence the method for vibration analysis can be fairly simplified.

ACKNOWLEDGEMENT

The authors wish to express their gratitude to Mr. S. Ito, Director of Compressor Division, Mr. S. Yamamura, Director of Engineering Section, Mr. M. Yamamura, Director of Engineering Development, Mr. K. Imasu, Chief Engineer of Air-conditioner Division and Mr. A. Shimizu, Engineer of Compressor Division, of Matsushita Electric Industrial Co., Ltd..

REFERENCES

1. Imaichi, K. et al., ASME Paper, 75-DET-44, 1975
2. Imaichi, K. et al., Proc. Purdue C.T.C., 1978, pp.283-288
3. Imaichi, K. et al., Proc. 15th Intr. Cong. Refrig., 1979, pp.727-733
4. Imaichi, K. et al., Proc. Purdue C.T.C., 1980, pp.90-96
5. Sommerfeld, A., Z. für Math. u. Phys., 50, 1904, pp.97.
6. Reynolds, O., Phil. Trans. Roy. Soc., 177, pt.1, 1886, pp.157